Genome-wide analysis of translational efficiency reveals distinct but overlapping functions of yeast DEAD-box RNA helicases Ded1 and eIF4A

Neelam Dabas Sen,[1] Fujun Zhou,[1] Nicholas T. Ingolia,[2] and Alan G. Hinnebusch[1]

[1]*Laboratory of Gene Regulation and Development, Eunice K. Shriver National Institute of Child Health and Human Development, National Institutes of Health, Bethesda, Maryland 20892, USA;* [2]*Department of Molecular and Cell Biology, University of California, Berkeley, California 94720, USA*

DEAD-box RNA helicases eIF4A and Ded1 are believed to promote translation initiation by resolving mRNA secondary structures that impede ribosome attachment at the mRNA 5′ end or subsequent scanning of the 5′ UTR, but whether they perform unique or overlapping functions in vivo is poorly understood. We compared the effects of mutations in Ded1 or eIF4A on global translational efficiencies (TEs) in budding yeast *Saccharomyces cerevisiae* by ribosome footprint profiling. Despite similar reductions in bulk translation, inactivation of a cold-sensitive Ded1 mutant substantially reduced the TEs of >600 mRNAs, whereas inactivation of a temperature-sensitive eIF4A variant encoded by *tif1–A79V* (in a strain lacking the ortholog *TIF2*) yielded <40 similarly impaired mRNAs. The broader requirement for Ded1 did not reflect more pervasive secondary structures at low temperature, as inactivation of temperature-sensitive and cold-sensitive *ded1* mutants gave highly correlated results. Interestingly, Ded1-dependent mRNAs exhibit greater than average 5′ UTR length and propensity for secondary structure, implicating Ded1 in scanning through structured 5′ UTRs. Reporter assays confirmed that cap-distal stem–loop insertions increase dependence on Ded1 but not eIF4A for efficient translation. While only a small fraction of mRNAs shows a heightened requirement for eIF4A, dependence on eIF4A is correlated with requirements for Ded1 and 5′ UTR features characteristic of Ded1-dependent mRNAs. Our findings suggest that Ded1 is critically required to promote scanning through secondary structures within 5′ UTRs, and while eIF4A cooperates with Ded1 in this function, it also promotes a step of initiation common to virtually all yeast mRNAs.

[Supplemental material is available for this article.]

In translation of most eukaryotic mRNAs, the initiation codon is selected by the scanning mechanism, wherein a 43S preinitiation complex (PIC) containing methionyl initiator tRNA (tRNA$_i$) attaches to the capped 5′ end of mRNA and scans the 5′ UTR for an AUG codon. PIC attachment to the mRNA is stimulated by eIF4F, comprised of cap-binding protein eIF4E, DExD/H-box helicase eIF4A, and scaffold subunit eIF4G, which stimulates eIF4A's ATP-dependent RNA helicase activity (Rogers et al. 2002; Schutz et al. 2008). Activation of eIF4A is expected to generate single-stranded RNA to facilitate ribosome binding, and mRNAs with more structured 5′ UTRs display a greater requirement for eIF4A/eIF4F (Blum et al. 1992; Svitkin et al. 2001; Pestova and Kolupaeva 2002; Mitchell et al. 2010). Interaction of eIF4G with components of the 43S complex, eIF3, eIF5, or eIF1, is thought to facilitate recruitment of the PIC to cap-bound eIF4F (for review, see Hinnebusch 2014).

As might be expected, eIF4F and ATP hydrolysis are dispensable in reconstituted systems for assembly of 48S PICs at the AUG codon on synthetic mRNAs with unstructured 5′ UTRs but are required with native mRNAs (Pestova et al. 1998; Pestova and Kolupaeva 2002; Mitchell et al. 2010). Moreover, inactivating eIF4A in mammalian extracts decreased translation of reporter mRNAs with cap-proximal structures by impairing eIF4F binding to mRNA and reducing 43S-mRNA attachment. However, translation of mRNAs devoid of structures was also reduced (Svitkin et al.

2001); similarly, translation of reporter mRNAs with only 8-nt-long 5′ UTRs was impaired in yeast extracts containing defective eIF4A variants (Blum et al. 1992). Thus, eIF4A helicase activity might be needed to dissociate RNA-RNA interactions other than stable stem–loops (SLs) or resolve mRNA-protein interactions in the 5′ UTR for efficient PIC attachment. Indeed, eIF4A is essential in yeast even though the 5′ UTRs of most yeast mRNAs are relatively short and devoid of highly stable, well-defined SLs (Ringner and Krogh 2005; Lawless et al. 2009; Kertesz et al. 2010; Wan et al. 2012; Rouskin et al. 2014).

In mammalian reconstituted systems, eIF4A can facilitate scanning through a SL of moderate stability distal from the cap (Pestova et al. 1996). Other DExD/H helicases, DHX29 and yeast Ded1 (the ortholog of mammalian DDX3X), were required with SLs of higher stability (Pisareva et al. 2008; Abaeva et al. 2011), although none (DHX29, DDX3X, or yeast Ded1) could substitute for eIF4F for 48S PIC assembly on beta-globin mRNA. Thus, it appeared that DHX29 and DDX3X/Ded1 specifically stimulate scanning through secondary structures, whereas eIF4F enhances both PIC attachment and scanning but is less effective in resolving strong SLs (Abaeva et al. 2011). In yeast cells, a *ded1* mutation had a stronger effect than an eIF4A mutation (*tif1-A79V* in a strain lacking *TIF2*) on translation of a reporter harboring a long 5′ UTR (Berthelot et al. 2004), and a *ded1* mutation impaired scanning

Corresponding authors: nick@ingolia.org; ahinnebusch@nih.gov
Article published online before print. Article, supplemental material, and publication date are at http://www.genome.org/cgi/doi/10.1101/gr.191601.115.

through a SL located distal to the 5′ cap (Chiu et al. 2010). On the other hand, inactivation of Ded1 in yeast (Chuang et al. 1997) or knock-down of *DHX29* in mammalian cells (Parsyan et al. 2009) impairs bulk translation, suggesting that DHX29 and Ded1 are not dedicated solely to mRNAs with strong, cap-distal secondary structures that impede scanning. The role of mammalian DDX3X in translation is not well understood (Lai et al. 2008; Lee et al. 2008), although recent work indicates that it resolves cap-proximal structures, possibly to facilitate eIF4F binding to the mRNA (Soto-Rifo et al. 2012), but it also can promote joining of 60S subunits to 48S PICs independent of helicase activity (Geissler et al. 2012).

DDX3X and Ded1 can function as translational repressors when present at abnormally high concentrations. Overexpressed DDX3X functioned as an inhibitory eIF4E-binding protein that competes with eIF4G for eIF4F assembly (Shih et al. 2008). Ded1 overexpression impairs yeast cell growth and induces assembly of stress granules; and excess Ded1 inhibits translation in cell extracts at the step of 48S PIC assembly. These inhibitory activities do not require Ded1 helicase activity. It was suggested that Ded1 interacts with eIF4G to assemble messenger ribonucleo-protein particles (mRNPs) that accumulate in stress granules and subsequently activates repressed mRNPs under favorable growth conditions through its helicase activity (Hilliker et al. 2011). Whereas Ded1 function in stimulating bulk translation is well established (Chuang et al. 1997; de la Cruz et al. 1997), it has not been shown that inactivating yeast Ded1 de-represses translation of mRNAs in unfavorable growth conditions. Clearly, additional work is needed to define the in vivo functions of Ded1 and DDX3X.

In this study, we sought to determine whether eIF4A and Ded1 perform largely overlapping functions or, rather, have distinct activities in stimulating translation initiation in living yeast cells. To this end, we conducted genome-wide ribosomal profiling (Ingolia et al. 2009) of *Saccharomyces cerevisiae* mutants defective for one or the other helicase under conditions where bulk translation is reduced, but not abolished, and identified mRNAs whose translational efficiencies are impaired to the greatest extent in each mutant.

Results

Ribosome footprint profiling of *ded1* mutants reveals sizable fractions of genes particularly dependent on Ded1 for efficient translation

To determine the relative importance of eIF4A and Ded1 in translation of different mRNAs, we constructed isogenic yeast strains containing the cold-sensitive (Cs⁻) allele *ded1-120*, encoding amino acid substitutions of Gly108/Gly494 with Asp (G108D/G494D), or the temperature-sensitive (Ts⁻) allele *ded1-952* (encoding substitutions T408I/W253R) as the only source of Ded1. G494D likely impairs conserved subdomain VI function in ATP binding or hydrolysis, whereas T408I in subdomain IV probably affects RNA binding (Linder and Jankowsky 2011). (Henceforth, these alleles are referred to as *ded1-cs* and *ded1-ts*.) We also constructed a strain lacking both chromosomal genes encoding eIF4A (*TIF1/TIF2*) and harboring the Ts⁻ allele *tif1-A79V* as the only source of eIF4A (*tif1-ts*), which confers a slow-growth phenotype (Slg⁻) at 30°C and lethality at 37°C. The location of A79V between subdomains Ib and Ic might indicate a defect in RNA binding (Linder and Jankowsky 2011). The growth defects of all

three mutants were fully complemented by the wild-type (WT) alleles on plasmids (Supplemental Fig. S1A–C).

To identify culture conditions that evoke comparable levels of translational inhibition in the mutants, polysome profiles were determined after shifting cultures to nonpermissive temperatures for different periods of time. For *ded1-cs* cells, marked dissociation of polysomes and accumulation of 80S monosomes were apparent after 10 min at 15°C, with the polysome:monosome (P/M) ratio reduced by ~77% compared to that seen in WT cells (Supplemental Fig. S1D). *ded1-ts* confers a relatively less severe defect, with a 2-h shift to 37°C required to reduce the P/M ratio by ~63% (Supplemental Fig. S1E). The P/M ratios of the *ded1* mutants at the permissive temperature were similar to those for the corresponding *DED1⁺* transformants (data not shown). For *tif1-ts*, the P/M ratio is ~75% below WT during continuous culture at 30°C (Supplemental Fig. S1F), consistent with its Slg⁻ phenotype at this temperature (Supplemental Fig. S1C); the P/M ratio was diminished further, for an ~83% reduction of the WT ratio, after 1 h at 37°C (Supplemental Fig. S1G).

We conducted ribosome profiling of the *ded1* and *tif1* strains and their WT counterparts under the conditions described in Supplemental Figure S1. Given that total polysomes are diminished in the mutants, the absolute translation efficiencies (TEs) of most mRNAs will be reduced in the mutant cells, but these reductions are masked by normalization to total ribosome footprint reads for each strain, such that changes in TE are calculated relative to all mRNAs. Those mRNAs exhibiting reductions in relative TE in mutant versus WT cells display a greater than average dependence on Ded1 or eIF4A for efficient translation in WT cells, whereas mRNAs exhibiting increased TE in the mutant show a lower than average dependence on the helicase. Both ribosome footprinting and RNA-seq results were highly reproducible between biological replicates for each strain (Pearson's $r \approx 0.99$) (Supplemental Fig. S2A–D). A scatterplot comparing ribosome footprint data between *ded1-cs* and WT cells revealed a population of genes with substantially altered translation in the mutant (Fig. 1A; red dots indicating >twofold deviation from identity), whereas RNA-seq data showed far fewer differences in mRNA abundance between the two strains (Fig. 1B), indicating widespread alterations in TE in *ded1-cs* cells (Fig. 1C).

Analysis of statistically significant changes in ribosome footprint or RNA-seq values revealed mRNA-specific changes in TE as the major consequence of reduced Ded1 activity. Ribosome footprint density was found to be significantly increased or decreased for 1026 of 4918 expressed genes analyzed (21%), whereas mRNA abundance levels were significantly changed for only 102 of 1026 affected genes. Integrating ribosome footprint and RNA-seq data revealed that 814 genes (~17% of expressed genes) displayed a change in TE in *ded1-cs* versus WT cells ($\Delta TE_{ded1-cs} = TE_{ded1-cs}/TE_{WT}$) of a factor of ≥ 2 with a false-discovery rate (FDR) of <0.01. A majority of these genes (617/814) displayed a reduction in TE in the mutant (Supplemental File S1), indicating that >10% of all genes exhibit a heightened dependence on Ded1 for efficient translation at 15°C.

Considering that RNA secondary structures should be more pervasive at lower temperatures, we asked whether Ded1 is also important for robust translation of many genes at elevated growth temperature by profiling the *ded1-ts* mutant shifted to 37°C (Supplemental Fig. S3A–D). A smaller fraction of all genes exhibited significant changes in TE in the *ded1-ts* mutant versus the *ded1-cs* strain (cf. Fig. 1D and 1C): Of 336 genes displaying a $\Delta TE_{ded1-ts}$ of $\geq$twofold, 228 (6.3% of expressed genes) were translated less
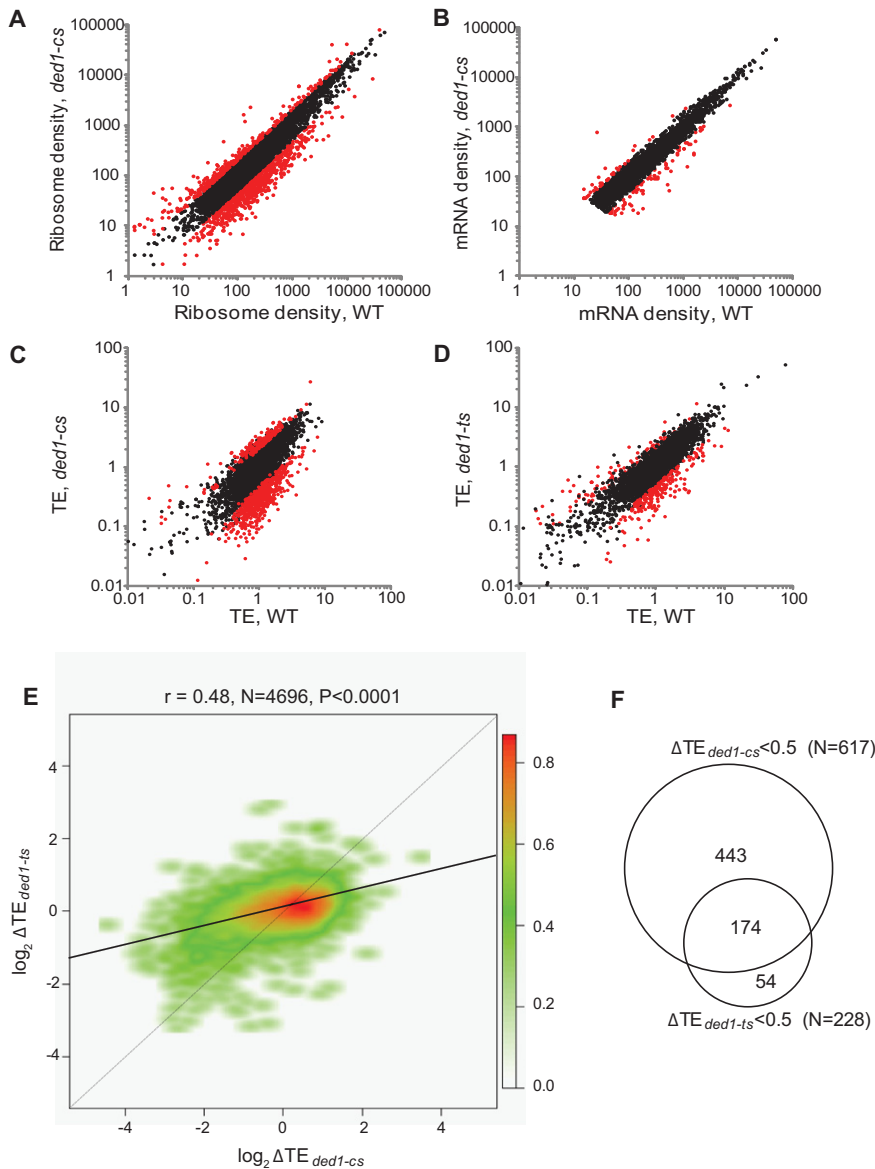
Figure 1. *ded1-cs* and *ded1-ts* mutations evoke genome-wide changes in relative TE values for substantial fractions of genes that overlap significantly. (*A,B*) Scatterplots of normalized read densities expressed as number of reads mapping to gene coding sequences normalized by coding sequence length and by total number of reads for that sample. (*A*) Ribosome footprint density and (*B*) mRNA density for *ded1-cs* (NSY5) versus WT (NSY4) strains. (*C*) Scatterplot of translational efficiencies (TEs) between WT and *ded1-cs*. Eight-hundred fourteen genes exhibiting ≥twofold changes in TE in *ded1-cs* cells at FDR < 0.01 are in red. (*D*) Same as *C* for WT (NSY10) versus *ded1-ts* (NSY11) strains; 336 genes with ≥twofold change in TE in *ded1-ts* cells at FDR < 0.01 colored red. (*E*) Smooth scatterplot of $\log_2\Delta$TE values for 4696 expressed genes for *ded1-ts* versus *ded1-cs* strains, excluding genes with $\log_2\Delta$TE >6 or <−6. Black line: determined regression line; gray line: theoretical regression line for identical changes in ΔTE values. Plot was generated using R smoothscatter function with 128 color bins and kernel density estimate. The red to green gradient indicates density of data points. (*F*) Venn diagram of overlap between genes exhibiting ≥twofold reductions in TE in the two *ded1* mutants.

efficiently in the mutant versus WT cells (Supplemental File S2). Nevertheless, there is extensive overlap between the genes exhibiting altered TE in *ded1-ts* versus *ded1-cs* cells, as the ΔTE_{ded1-ts} and ΔTE_{ded1-cs} values for all genes are significantly correlated (Pearson's $r = 0.48$, $P < 0.0001$) (Fig. 1E). Moreover, the majority (76%) of genes exhibiting ≥twofold reductions in TE in *ded1-ts* cells were similarly down-regulated in the *ded1-cs* strain (Fig. 1F).

Consistent with the relative effects of the two mutations on bulk translation (Supplemental Fig. S1D,E), the magnitude of ΔTE values genome-wide is greater for *ded1-cs* versus *ded1-ts* cells, as revealed by a slope <1 for the trend-line of the scatterplot ΔTE_{ded1-ts} versus ΔTE_{ded1-cs} (Fig. 1E). Thus, a sizable fraction of genes display a marked dependence on Ded1 for efficient translation at both elevated and reduced growth temperatures.

Ribosome footprint profiling reveals only a small fraction of genes particularly dependent on eIF4A for efficient translation

Ribosome profiling of the *tif1-ts* mutant and isogenic WT strain cultured continuously at 30°C, and following a shift from 30°C to 37°C (Supplemental Fig. S4A–H), gave results distinct from those described for *ded1* mutants. At 30°C, 211 genes displayed significantly altered ribosome densities (55 genes decreased and 156 genes increased) in the *tif1-ts* mutant versus WT strain, but most of these changes were accompanied by a corresponding change in mRNA abundance (Supplemental File S3). On a shift to 37°C, ribosome density was significantly altered in the *tif1-ts* mutant for 123 genes, and this alteration occurred at the translational level for roughly half (68 genes with >twofold change in TE at FDR < 0.01), of which only 36 (0.72% of all expressed genes) displayed a significant reduction in TE (Fig. 2A). Thus, in contrast to results above for Ded1, only a small proportion of genes display a substantially greater than average dependence on eIF4A for efficient translation at 37°C.

Twelve of the 36 genes whose TE was decreased by >twofold in *tif1-ts* cells at 37°C were similarly affected in *ded1-cs* cells (Fig. 2B), which is ∼2.5-fold higher than the ∼five such genes expected from chance alone (36·[605/4696] = 4.6). Furthermore, analysis of all expressed genes revealed that the ΔTE values for *tif1-ts* versus WT cells at 37°C (ΔTE_{tif1-ts(37)}) are significantly correlated with ΔTE values for both *ded1-cs* cells and *ded1-ts* cells (r values of 0.27 and 0.39, respectively) (Fig. 2C; Table 1). However, the magnitude of TE changes genome-wide is considerably larger in *ded1-cs* versus *tif1-ts* cells (Fig. 2C). The degree of functional overlap between Ded1 and eIF4A is illustrated by the gene clustering analysis in Figure 2D. Among major clusters discerned, clusters 1–3 tend to show increased TEs, while clusters 7–9 generally exhibit reduced TEs in the two *ded1* mutants and *tif1-ts* cells. In contrast, genes in
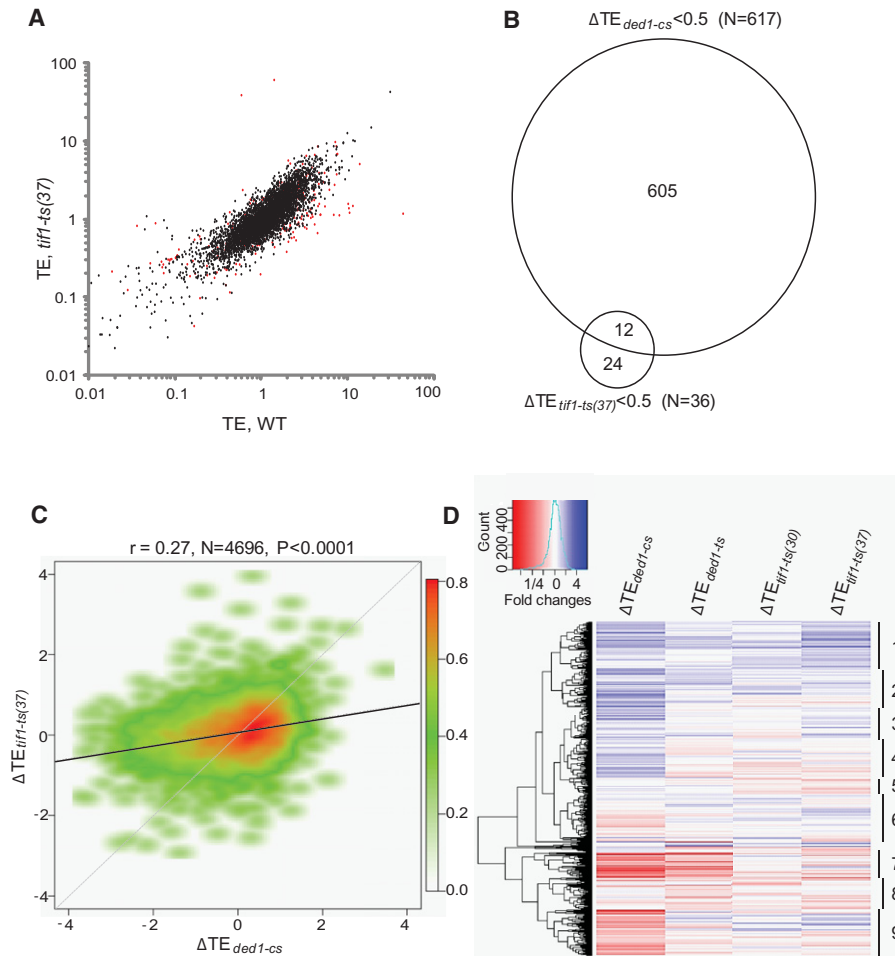
Figure 2. A significant number of genes require both Ded1 and eIF4A for WT translation. (*A*) Scatterplot of TE of *tif1-ts* versus WT cells at 37°C, with 68 genes showing a ≥twofold change in the mutant at FDR < 0.01, colored red. (*B*) Venn diagram of genes exhibiting ≥twofold reductions in *tif1-ts* (at 37°C) and *ded1-cs* strains. (*C*) Smooth scatterplot of the indicated $\log_2$ ΔTE values, generated as in Figure 1E. (*D*) Hierarchical clustering analysis of absolute ΔTE values for 4696 expressed genes from the indicated mutant versus WT comparisons (excluding genes with >64-fold changes in TE) as a heat map using the R heatmap.2 function from the R "gplots" library, using the default hclust hierarchical clustering algorithm.

and are resolved by the Ded1 helicase function. To test this, we interrogated the 5′ UTRs of Ded1-dependent mRNAs using a compilation of 5′ UTR lengths and propensities for secondary structure for 3000 yeast genes (Kertesz et al. 2010). Interestingly, the 328 genes with a ≥twofold reduction in TE in *ded1-cs* cells (for which 5′ UTRs were compiled) exhibit a mean 5′ UTR length of 149 nt, substantially greater than the mean 5′ UTR length of 79 nt calculated for all 2593 compiled genes examined in our study ($P < 0.0001$) (Fig. 3A). Moreover, the 129 genes (out of 197 compiled) displaying a ≥twofold increase in TE in *ded1-cs* cells have a mean 5′ UTR length of only 45 nt, significantly smaller than the genome-average 5′ UTR length ($P < 0.0001$) (Fig. 3A). Thus, mRNAs with greater than average dependence on Ded1 tend to have atypically long 5′ UTRs.

To determine whether Ded1-dependence is associated with elevated secondary structure, we interrogated the same data set (Kertesz et al. 2010) wherein each transcribed nucleotide in 3000 different yeast transcripts was assigned a "parallel analysis of RNA structure" (PARS) score, based on its susceptibility in yeast mRNA reannealed in vitro to digestion with nucleases specific for single-stranded or double-stranded RNA, with a higher PARS score denoting a higher frequency of residing in double-stranded conformation. For each transcript we examined: sum of PARS scores for all 5′ UTR nucleotides (Total PARS); average PARS score over the 5′ UTR (Avg PARS); sum of PARS scores for the first 30 nt (First30 PARS); sum of PARS scores for 30 nt surrounding the start codon (for genes with a 5′ UTR of ≥15 nt; Start30 PARS); and highest total PARS score measured in any 30-nt window sliding across the 5′ UTR (Max30 PARS) (Fig. 3B). We also tabulated PARS scores downstream from the AUG, including intervals +1 to +30 (Plus15), +16 to +45 (Plus30), +31 to +60 (Plus45), +46 to +75 (Plus60), and +61 to +90 (Plus75).

clusters 4–6 display differential responses in different mutants. Together, our results indicate that (1) there are many genes that display a greater than average requirement for both Ded1 and eIF4A and are affected to a greater extent by inactivating Ded1 versus eIF4A; but also that (2) many genes have a greater than average dependence on one helicase but not the other; and (3) only a small fraction of genes exhibit a strong dependence on eIF4A. To account for these conclusions, we propose that most mRNAs exhibit a similar dependence on eIF4A for binding eIF4F or PIC attachment to the mRNA 5′ end, while a sizable proportion are unusually dependent on Ded1 because they harbor secondary structures that impede scanning, which are resolved primarily by Ded1 with auxiliary contributions from eIF4A.

The 5′ UTRs of Ded1-dependent mRNAs are atypically long with greater than average propensity for secondary structure

A prediction of our interpretation is that Ded1-dependent mRNAs should exhibit distinctive structural features that impede scanning

Table 1. Correlation between translational changes in *ded1* or *tif1* mutant versus WT cells for all 4696 expressed genes

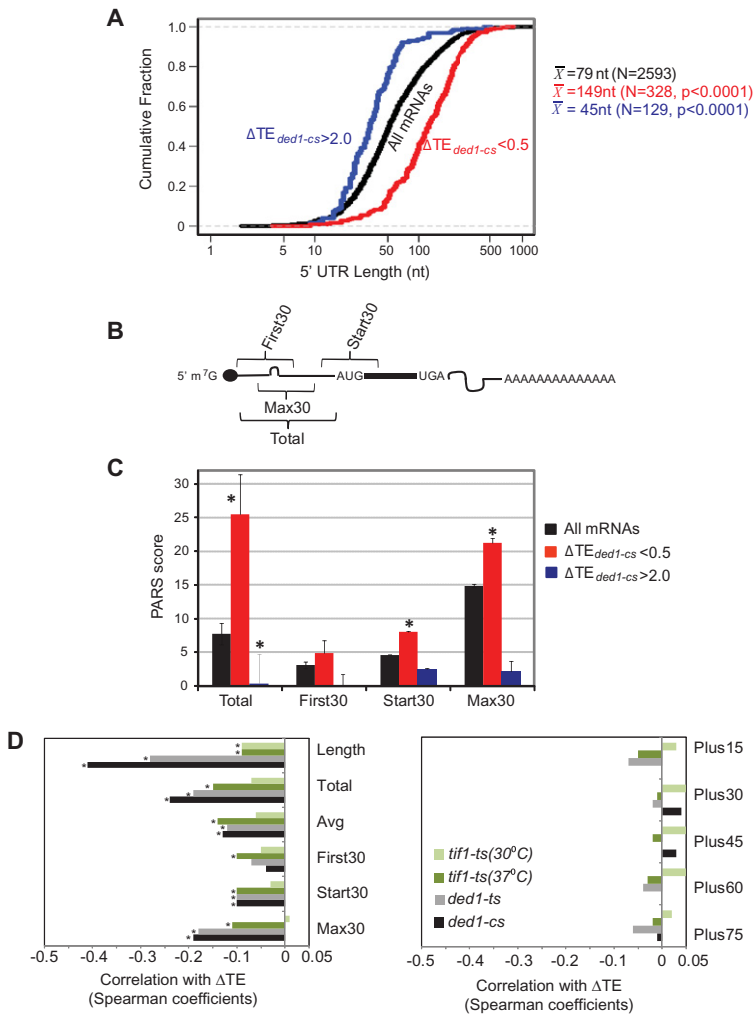|	Pearson correlation coefficient (*r*)		
	$\mathbf{\Delta TE}_{ded1-ts}$	$\mathbf{\Delta TE}_{tif1-ts(30)}$	$\mathbf{\Delta TE}_{tif1-ts(37)}$
$\Delta TE_{ded1-cs}$	0.48(***)	0.11(***)	0.27(***)
$\Delta TE_{ded1-ts}$		0.21(***)	0.39(***)
$\Delta TE_{tif1-ts(30)}$			0.39(***)

(***) $P < 0.0001$.

Figure 3. 5′ UTRs of Ded1-dependent genes exhibit greater than average length and PARS scores. 5′ UTR features of genes with ≥twofold reductions in TE in *ded1-cs* cells, for genes curated by Kertesz et al. (2010). (*A*) Cumulative distributions of 5′ UTR lengths for all 2593 genes, or genes of indicated ΔTE values, with mean lengths (X) for the indicated number of genes (N). *P*-values of Student's *t*-tests for statistical significance of the differences between mean lengths for Ded1-dependent genes and genome-average length (79 nt) are shown. (*B*) Schematic showing 5′ UTR intervals assigned for calculating cumulative PARS scores. (*C*) Average PARS scores calculated for the indicated gene set for each 5′ UTR interval described in *B*. (*) $P < 0.05$. (*D*) Genome-wide changes in TE are negatively correlated with 5′ UTR length and PARS scores in *ded1* and *tif1* mutants. Spearman correlation coefficients of ΔTE values in the indicated mutant versus WT cells for the 5′ UTR features described in *B* and the text. Coefficients with significance levels of $P < 10^{-16}$ are indicated with asterisks.

Remarkably, for 328/617 genes annotated with PARS scores and displaying $\Delta TE_{ded1-cs} < 0.5$, all 5′ UTR PARS features, but none for coding sequences, were significantly greater than the genome averages for all 2593 transcripts in the PARS database (Fig. 3C; Table 2, cf. columns 2 and 3). In contrast, for 129 genes with $\Delta TE_{ded1-cs} > 2$, none of the PARS features were atypical except that the 5′ UTR Total PARS score was considerably lower than the genome average (Fig. 3C; Table 2, cf. columns 2 and 5). Similar conclusions were reached from genome-wide analysis of correlations between ΔTE and 5′ UTR length or PARS features in *ded1-cs* cells, as significant Spearman (negative) correlation coefficients were observed for all 5′ UTR features except for the First30 PARS score (Fig. 3D, left, black bars) but for none of the coding sequence features (Fig. 3D, right, black bars). The strongest negative correla-

tions with $\Delta TE_{ded1-cs}$ values were for length, Total PARS, and Max30 PARS scores of 5′ UTRs (Fig. 3D, left). Analysis of genes showing $\Delta TE_{ded1-ts} < 0.5$ (Supplemental Table S1) and genome-wide correlation analyses conducted for the *ded1-ts* mutant revealed similar conclusions (Fig. 3D, gray bars). These findings suggest that 5′ UTR length and propensity for secondary structure make significant contributions to changes in TE evoked by *ded1-cs* and *ded1-ts* mutations.

For *tif1-ts* cells at 37°C, significant but weaker negative correlations were observed between ΔTE values and all 5′ UTR parameters, with the strongest correlations for total PARS, average PARS, and Max30 PARS scores (Fig. 3D, dark olive). ΔTE values for *tif1-ts* cells at 30°C displayed even weaker negative correlations with these same three 5′ UTR features (Fig. 3D, lime). Thus, a propensity for secondary structure in the 5′ UTR is a significant determinant of diminished TE evoked by impairing eIF4A function, but this characteristic is less predictive of changes in TE than is the case with comparable reductions in Ded1 activity.

Interestingly, as described in Supplemental Figure S5, gene ontology (GO) analysis of genes exhibiting reduced TE in *ded1* or *tif1* mutants indicated that Ded1, but not eIF4A, is particularly important for efficient translation of certain genes involved in cell growth, polarity, or morphogenesis; whereas a group of genes concerned with DNA topology, DNA damage response, chromosome structure, or mitotic recombination display a diminished dependence on eIF4A.

Identification of 5′ UTRs that confer Ded1 dependence

We next sought to identify genes for which sequences conferring unusual dependence on Ded1 are confined to the 5′ UTR by fusing promoters and 5′ UTRs of candidate genes to firefly luciferase coding sequences (*FLUC*) and a truncated version of the 3′ UTR of yeast *RPL41A* (Fig. 4A). Eleven candidate genes were examined that exhibit a >threefold decrease in TE as well as abundant mRNA levels that do not change appreciably in *ded1-cs* cells. We also included three genes identified in a recent genome-wide analysis of stable secondary structures in yeast cells containing well-defined SL structures confined to the 5′ UTR: *SFT2*, *PMA1*, and *PCL5* (Rouskin et al. 2014), which displayed $\Delta TE_{ded1-cs}$ values of ~0.25–0.3. As controls, *LUC* reporters were constructed for eight genes whose TEs were either not substantially reduced, or increased, in the *ded1-cs* mutant. Luciferase expression was assayed after incubating the *ded1-cs* mutant and WT transformants at 23°C, where *ded1-cs* cells continue to divide but

Table 2. Comparison of 5′ UTR lengths and PARS features for genes exhibiting significant TE changes in *ded1-cs* mutant versus WT cells

5′ UTR feature	All mRNAs ($n = 2593$)	$\Delta TE_{ded1-cs} < 0.5$		$\Delta TE_{ded1-cs} > 2$	
		($n = 328$)	P value	($n = 129$)	P value
Total length	79.0 ± 1.6	149 ± 5.9	<0.0001	45.3 ± 4.42	<0.0001
Total PARS	7.76 ± 0.49	25.5 ± 1.88	<0.0001	0.393 ± 1.74	0.001
Average PARS	0.058 ± 0.008	0.181 ± 0.02	<0.0001	0.0016 ± 0.048	0.16
First30 PARS	3.12 ± 0.27	4.92 ± 0.68	0.02	2.54 ± 1.5	0.64
Start30 PARS	4.61 ± 0.32	8.08 ± 0.77	<0.0001	2.18 ± 1.92	0.10
Max30 PARS	14.9 ± 0.32	21.2 ± 0.85	<0.0001	12.1 ± 1.63	0.07
Plus15 PARS	9.15 ± 0.31	9.26 ± 0.69	0.90	9.31 ± 2.04	0.91
Plus30 PARS	8.83 ± 0.33	8.41 ± 0.74	0.66	11.8 ± 1.93	0.06
Plus45 PARS	9.04 ± 0.33	8.6 ± 0.73	0.65	12.5 ± 2.07	0.03
Plus60 PARS	9.41 ± 0.32	9.71 ± 0.78	0.76	10.5 ± 1.76	0.49
Plus75 PARS	9.65 ± 0.33	11.0 ± 0.79	0.16	10.4 ± 1.64	0.61

Mean (±SEM) 5′ UTR length in nucleotides or indicated PARS feature (defined in Fig. 3B) was calculated from the database compiled in Kertesz et al. (2010) for all 2593 genes, or the sets of 328 or 129 genes satisfying the indicated $\Delta TE_{ded1-cs}$ criteria.

exhibit a slow-growth phenotype. (We chose continuous culture at a semipermissive temperature versus shift to the nonpermissive temperature of 15°C to overcome the complication of detecting luciferase produced in mutant cells in the permissive condition. Whereas dilution of the pre-existing luciferase would be prevented by cessation of cell division at 15°C, it would occur at 23°C where mutant cells still divide.)

We observed a significant reduction in LUC expression in the *ded1-cs* mutant for 12 of 14 reporters containing 5′ UTRs of Ded1-dependent genes, including *PMA1* and *PCL5* that harbor defined SLs in their 5′ UTRs, whereas none of the control reporters exhibited a significant decrease, and several displayed increased LUC expression in *ded1-cs* versus WT cells (Supplemental Table S2). A plot of the changes in LUC expression against changes in ribosome density reveals significant correlation between these parameters (Fig. 4B). However, six of the 14 reporters for Ded1-dependent genes displayed reductions in LUC expression in *ded1-cs* cells considerably smaller than the reductions in ribosome density observed for the corresponding native genes (*YPR159W*, *YNL101W*, *YIL090W*, *YDL145C*, *YML035C*, and *YBL102W*) (Supplemental Table S2). One possible explanation for this discrepancy is that Ded1 function is relatively less impaired in *ded1-cs* cells at the 23°C temperature used for reporter assays versus the 15°C temperature used for ribosome profiling (data not shown). In fact, 5/6 Ded1-dependent genes showing the least correspondence between LUC expression and ribosome density have relatively low Total PARS and Max30 PARS scores compared to other Ded1-dependent genes subjected to reporter analysis (Supplemental Table S2), such that Ded1 function remaining at 23°C in *ded1-cs* cells might be sufficient to overcome the moderately stable structures formed by these 5′ UTRs. Another possibility is that the 5′ UTRs of some of these mRNAs could engage in long-range interactions with their CDS or 3′ UTRs, forming inhibitory structures that would be absent in the corresponding *LUC* reporter constructs. These interactions might be underrepresented in PARS analysis of purified mRNAs folded in vitro if they are stimulated in vivo by eIF4G interactions with poly(A)-binding protein that juxtapose mRNA 5′ and 3′ ends.

Ded1 is critically required for scanning through a cap-distal SL structure

Our ribosomal profiling results indicated that 5′ UTRs of mRNAs displaying strong Ded1 dependence tend to be atypically long

and conducive to secondary structure. Previous studies indicated that inactivation of Ded1 in yeast cells reduces translation of reporter constructs containing long 5′ UTRs (Berthelot et al. 2004) or harboring a SL insertion (Chiu et al. 2010); however, the relative contributions of length and secondary structure, and the importance of SL position in the 5′ UTR, were unclear. Hence, we assayed a panel of *LUC* reporters in which the length of an unstructured 5′ UTR and position and stability of SL insertions were varied systematically, using the same strains and semipermissive growth
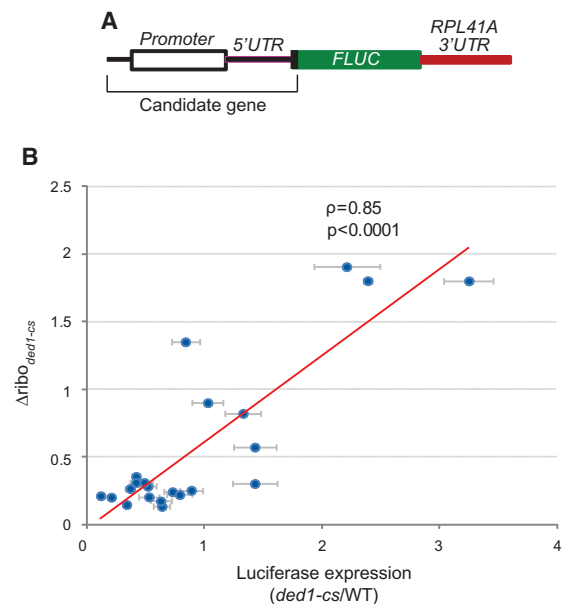

Figure 4. Identification of 5′ UTRs sufficient to confer Ded1 dependence of *LUC* reporter expression. (*A*) Schematic of reporters containing promoter, 5′ UTR, and first 20 codons of candidate genes, fused to firefly luciferase coding sequences (*FLUC*) and a modified *RPL41A* 3′ UTR. (*B*) Changes in ribosome density of the 22 candidate genes (from ribosome footprints) in *ded1-cs* versus WT cells plotted against the ratio of LUC expression in *ded1-cs* versus WT for corresponding reporters. Strains were grown in SC −Leu−Ura at 30°C, diluted to OD_{600}~0.1, and grown for ~three doublings at 23°C (~18 h for *ded1-cs* and ~10 h for WT). Luciferase activities were assayed in whole cell extracts (WCE), normalized to total protein, and reported in relative light units (RLUs) per mg of protein, as means (±SEM) determined from six transformants.

conditions as above. The reporters contain the promoter, the 22-nt 5' UTR, and the first four codons of *RPL41A* fused to *LUC* and the truncated *RPL41A* 3' UTR, with CAA repeats inserted into the 5' UTR to vary its length without increasing secondary structure. Sequences capable of forming SLs of varying stabilities were inserted into the construct with a 91-nt 5' UTR, 7 nt or 55 nt from the mRNA 5' end (Fig. 5A,B). As 43S PICs protect ~45 nt of mRNA (Kozak and Shatkin 1977; Lazarowitz and Robertson 1977), the cap-proximal SLs inserted 7 nt from the 5' end should inhibit 43S PIC attachment, whereas cap-distal SL insertions at 55 nt should inhibit scanning through the 5' UTR without impeding 43S attachment.

Figure 5. Cap-distal, but not cap-proximal, SL insertion confers strong Ded1 dependence on *LUC* reporter expression. (*A*) Schematics of *LUC* reporters containing promoter, 22-nt 5' UTR, and first four codons of *RPL41A* fused to *FLUC* coding sequences and modified *RPL41A* 3' UTR, plus indicated 5' UTR insertions of CAA repeats. LUC expression was assayed as in Figure 4B and mean (±SEM) ratios of expression in *ded1-cs* versus WT cells are plotted. (*B*) Schematics to indicate the position and stability of SLs (predicted at http://rna.urmc.rochester.edu/RNAstructure.html) inserted into the 91-nt 5' UTR reporter in *A*. LUC expression was assayed as in Figure 4B; and mean (±SEM) expression (in million units) in WT (*middle*) and ratios of expression in *ded1-cs* versus WT cells (*right*) are plotted. (*C*) Same as *B* except that LUC expression was measured in three transformants of WT and *tif1-ts* by preculturing in SC–Leu–Ura at 23°C, diluting to OD$_{600}$~0.1, and growing for ~three doublings at 33°C (~24 h for *tif1-ts* and ~6 h for WT).

Increasing the 5' UTR length from 22 nt to 187 nt had little effect on LUC expression in WT cells, and expression of all four reporter constructs of this category was reduced in *ded1-cs* cells by similar amounts, to ~80% of the WT level (Fig. 5A), indicating that lengthening the 5' UTR per se does not increase Ded1 dependence. A cap-distal insertion of moderate predicted stability (−3.7 kcal/mol) drastically inhibited luciferase expression in WT cells, whereas a cap-proximal insertion of higher predicted stability (−10.5 kcal/mol) was required for a comparable reduction in reporter expression (WT, 23°C) (Fig. 5B). Remarkably, the −3.7 kcal/mol cap-distal insertion conferred a strong requirement for Ded1, greatly reducing the *ded1*-cs/WT expression ratio, whereas the −10.5 kcal/mol cap-proximal insertion produced a small increase in Ded1 dependence comparable to that seen for cap-distal insertions of lower predicted stabilities (Fig. 5B, rightmost panel). These findings suggest that Ded1 is more critically required for translation of an mRNA harboring a cap-distal SL versus one with a cap-proximal SL, consistent with a greater requirement for Ded1 in scanning through secondary structures versus 43S attachment near the 5' end. The tendency for Ded1-dependent genes to have longer than average 5' UTRs might partly reflect the fact that longer 5' UTRs have greater numbers of nucleotides capable of forming structures that impede scanning.

To confirm that the reduced LUC expression in *ded1-cs* cells conferred by the −3.7 kcal/mol cap-distal SL reflected diminished translation initiation, we determined the distribution of this "SL-mRNA" between polysomes, monosomes, 40S subunits, and free mRNPs resolved by sedimentation of whole cell extracts (WCE) through sucrose density gradients. Cells were treated with formaldehyde prior to harvesting to fix 48S PICs and polysomes and prevent their dissociation during sedimentation. As expected, total polysomes were depleted in the *ded1-cs* mutant compared to WT (Fig. 6A), and the reporter mRNA containing the extended 5' UTR but no SL insertion was associated with large polysomes in both the mutant and WT but shifted somewhat toward smaller polysomes in the *ded1-cs* mutant (Fig. 6B, left). In both WT and *ded1-cs* cells, the SL-mRNA was shifted to smaller polysomes, monosomes, and 48S PICs compared to the no-SL mRNA (Fig. 6B, cf. right and left panels), in accordance with reduced expression of the SL-containing reporter in both strains (Fig. 5B). Importantly, the proportion of SL-mRNA in large polysomes is decreased with an attendant increase in the proportion present in the 48S fraction in *ded1-cs* versus WT cells
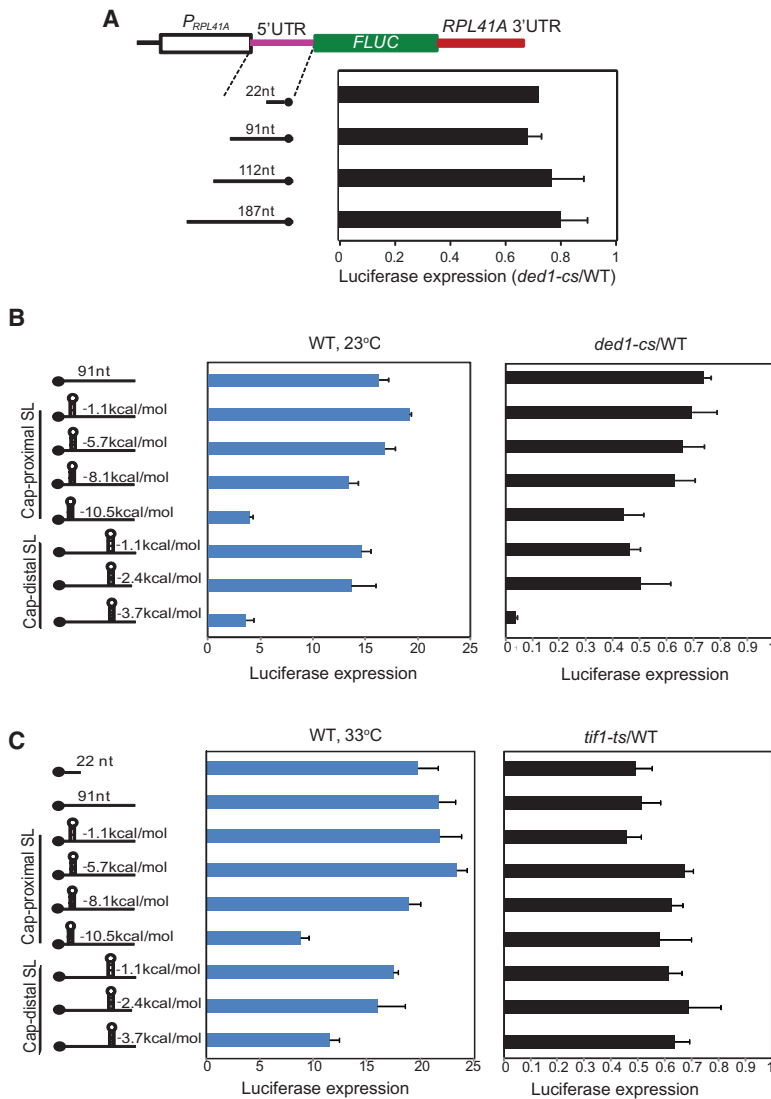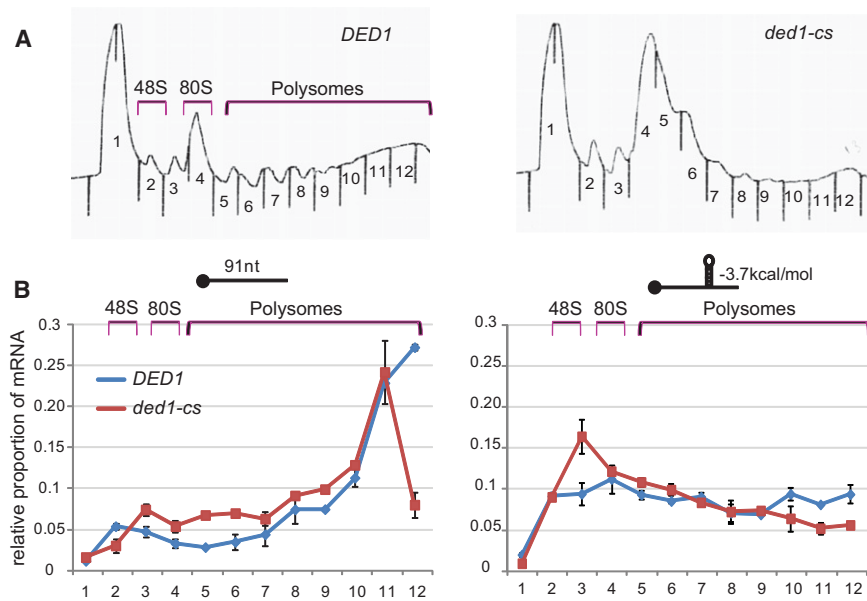
Figure 6. Inactivation of Ded1 evokes accumulation in 48S PICs of *LUC* reporter mRNA with a stable cap-distal SL insertion. (*A*,*B*) WT and *ded1-cs* strains harboring *LUC* reporters described in Figure 5A,B, with a 91-nt 5′ UTR or containing the −3.7 kcal/mol SL, were cultured as in Figure 4B and cells were cross-linked with 2% HCHO for 1 h prior to harvesting. WCEs were resolved by sedimentation through 10%–50% sucrose gradients, and fractions were collected while scanning at 254 nm. (*A*) Representative polysome profiles. (*B*) Gradient fractions were spiked with equal amounts of control RNA, total RNA extracted, and abundance of *LUC* reporter (relative to control) mRNA quantified by qRT-PCR, conducting three technical replicates for each fraction. Results from biological replicates ±SEM are shown.

Discussion

We have used a combination of ribosome profiling and reporter analysis to shed light on the in vivo functions of Ded1 and eIF4A in translation of different mRNAs in yeast. Because both helicases are essential, and mutations in either protein reduce bulk translation initiation, we sought to determine whether the sets of mRNAs that are most dependent on Ded1 or eIF4A overlap extensively or, rather, are largely nonoverlapping and exhibit distinct properties. Our findings suggest an outcome somewhere between these extremes. Inactivation of Ded1 by the *ded1-cs* mutation led to widespread reductions in TEs of many mRNAs, which exhibit a mean 5′ UTR length about twice the genome average, and a heightened propensity for secondary structures (higher PARS scores). Conversely, genes displaying ≥twofold increased TE in *ded1-cs* cells exhibit mean 5′ UTR length and PARS scores below genome averages. We also identified inverse correlations genome-wide between changes in TE and the length and PARS features of 5′ UTRs for both *ded1-cs* and *ded1-ts* mutants. These results support the notion that Ded1 is important for stimulating 43S PIC scanning through 5′ UTRs of many yeast mRNAs.

The stimulatory effect of Ded1 could involve increased processivity or a greater ability to resolve secondary structures. Analysis of *LUC* reporters with unstructured 5′ UTRs indicate that a longer 5′ UTR per se does not confer greater Ded1 dependence, inconsistent with Ded1 simply preventing PIC drop-off during scanning through long distances. In contrast, insertion of a SL of moderate stability 55 nt from the cap, where it should affect scanning but not PIC attachment, dramatically increased the effect of *ded1-cs* on reporter expression, and this SL-mRNA was shifted from polysomes/monsomes into 48S PICs in the mutant cells, consistent with scanning PICs becoming paused at the SL. Insertion of a strong SL only 7 nt from the cap produced a moderate increase in Ded1 dependence, suggesting that Ded1 also promotes 43S PIC attachment at the 5′ ends of mRNAs harboring cap-proximal secondary structure. One way to explain the relatively smaller Ded1 dependence of the reporter with cap-proximal SL is to propose that Ded1 and eIF4A make comparable contributions to PIC attachment at 5′ ends, whereas Ded1 is paramount in resolving cap-distal structures. This would account for genetic data suggesting that Ded1 functionally overlaps with eIF4F in yeast cells (de la Cruz et al. 1997), as well as previous findings that inactivating Ded1, but not eIF4A, specifically impaired expression of a reporter with a long 5′ UTR relative to one with a more typical short 5′ UTR (Berthelot et al. 2004). We suggest that the increased Ded1 dependence of the long-5′ UTR reporter in that study reflected the use of the *GCN4* mRNA leader, which is not devoid of structure, such that the longer 5′ UTR contained more structure-forming sequences that impede scanning and can be resolved by Ded1. We advance the same interpretation to account for the inverse correlation

(Fig. 6B, right). This shift in distribution is consistent with reduced translation and accumulation of the SL-mRNA in 48S intermediates with a scanning PIC stalled at the SL insertion. As described in Supplemental Figure S6, omitting formaldehyde fixation led to accumulation of SL-mRNA at the top of gradient instead of the 48S region for the *ded1-cs* extracts, ruling out accumulation of free mRNP versus 48S PICs in the experiment of Figure 6B.

Having found by ribosome profiling that relatively few mRNAs show a greater than average dependence on eIF4A, we examined the effects of the *tif1-ts* mutation on expression of the same *LUC* reporters at 33°C. In WT cells, the SL insertions reduced reporter expression (Fig. 5C, left) similarly to that described above at 23°C (Fig. 5B, left), except that the magnitude of inhibition was diminished at the higher temperature of 33°C. Surprisingly, in *tif1-ts* cells, *LUC* reporter expression was reduced by 40%–50% regardless of the presence or location of a SL structure, indicating that the SLs did not increase dependence on eIF4A for efficient translation. Similar results were obtained when WT and *tif1-ts* cells were cultured at 30°C (Supplemental Fig. S7). As described in Supplemental Figure S8, we obtained additional evidence corroborating our conclusion that cap-distal secondary structures increase dependence on Ded1, but not eIF4A, for translation in vivo by assaying *GCN4-lacZ* reporters containing or lacking a cap-distal SL. Finally, Supplemental Figure S9 presents results obtained on the *ded1-ts* mutant assayed at 33°C demonstrating that the stronger effect of *ded1-cs* versus *tif1-ts* on expression of the *LUC* reporter with cap-distal SL did not result from the fact that *ded1-cs* cells were examined at 23°C (Fig. 5B) where the SL should be more stable than at the 33°C temperature used to inactivate *tif1-ts* (Fig. 5C). We conclude that efficient translation in the presence of a cap-distal SL is more strongly dependent on Ded1 than eIF4A in cells regardless of the growth temperature.

observed here between changes in TE and 5′ UTR length in *ded1* mutant cells.

As noted earlier, previous studies showed that overexpressed Ded1 inhibits translation (Beckham et al. 2008) and accumulates in stress granules in yeast cells and that these inhibitory effects are enhanced by inactivation of its ATPase activity, leading to the model that Ded1 assembles translationally repressed mRNPs and can reverse the repression under the appropriate conditions through its helicase function (Hilliker et al. 2011). While it is still unclear whether Ded1 at native levels can repress translation, some mRNAs that display reduced TEs in the *ded1* mutants might be translationally repressed by the mutant Ded1 proteins rather than be impaired by the absence of Ded1 helicase activity. Examining the effects of mutant Ded1 proteins on translation of such mRNAs in a reconstituted system might resolve this issue.

Our genome-wide analysis of the effects of inactivating eIF4A by the *tif1-ts* mutation identified ~20-fold fewer genes than the number of Ded1-dependent genes identified in *ded1-cs* cells at 15°C, despite comparable reductions in bulk polysome assembly in the two mutants. These findings suggest that most yeast mRNAs have comparable requirements for eIF4A and are thus similarly impaired in the *tif1-ts* mutant. This conclusion is mirrored by our findings that the presence of stable SL insertions in the 5′ UTR increased the deleterious effect of *ded1-cs,* but not *tif1-ts,* on reporter expression in vivo. Interestingly, approximately one-third of the unusually eIF4A-dependent genes also strongly depend on Ded1, and there is a positive correlation between the effects of *tif1-ts* and *ded1-cs* on TEs genome-wide. Consistently, changes in TE are negatively correlated with length and PARS features of 5′ UTRs in the *tif1-ts* mutant, as in the *ded1* mutants. These findings suggest that a substantial proportion of mRNAs displaying atypical dependence on Ded1 also exhibit an enhanced requirement for eIF4A, of lesser magnitude. Many of the mRNAs with this dual Ded1/eIF4A requirement are visible in gene clusters 7–9 of the heat map in Figure 2D. This overlap between Ded1- and eIF4A-dependent mRNAs, together with the moderate tendency for eIF4A-dependent mRNAs to have longer, more structured 5′ UTRs, suggests that eIF4A and Ded1 functionally cooperate on a subset of mRNAs to promote scanning through 5′ UTRs, with Ded1 generally making the stronger contribution to resolving cap-distal secondary structures. The cluster analysis also reveals genes with a greater than average dependence on Ded1, whose relative TE actually increases in the *tif1-ts* mutant (e.g., cluster 6), signifying a smaller than average dependence on eIF4A function; the converse is evident for many genes in clusters 4–5 (Fig. 2D). Thus, there appear to be subsets of mRNAs in which one helicase but not the other makes an important contribution to TE. The mRNAs that exhibit a greater requirement for eIF4A than Ded1 might have a cap-proximal sequence or structure that impedes eIF4F attachment to the mRNA, which would depend largely on eIF4A functioning as a component of eIF4F.

Results from the *ded1-ts* mutant indicate that our identification of many fewer mRNAs strongly dependent on eIF4A versus Ded1 is unlikely due to the lower incubation temperature for *ded1-cs*. We also considered whether we had underestimated the number of genes strongly dependent on eIF4A because reductions in ribosome occupancy conferred by *tif1-ts* evoked increased mRNA turnover and reduced mRNA abundance, a secondary effect that could dampen calculated reductions in TE. Indeed, there is a strong correlation between changes in ribosome occupancy and changes in mRNA abundance genome-wide in the *tif1-ts* mutant at both 30°C and 37°C (Spearman coefficients, $\rho = 0.52$ and $\rho =$

0.45, respectively). However, we found an equally strong correlation between changes in ribosome occupancy and mRNA levels in the *ded1-ts* mutant ($\rho = 0.52$), while analysis of the *ded1-ts* and *tif1-ts* mutants identified ~sixfold more genes strongly dependent on Ded1 versus eIF4A at the same incubation temperature. Note also that many more genes exhibit ≥twofold changes in ribosome occupancy (ΔRibo) in the *ded1-cs* and *ded1-ts* strains (1026 and 749 genes, respectively) versus the *tif1-ts* mutant at 30°C or 37°C (211 and 123 genes, respectively). Thus, even if all changes in ribosome occupancy in *tif1-ts* cells resulted from altered translation rates (regardless of whether they are accompanied by changes in mRNA abundance), there would still be many fewer genes strongly affected in *tif1-ts* versus *ded1-ts* or *ded1-cs* cells, as we concluded from analyzing changes in TE.

The increased dependence on Ded1 imparted by 5′ UTR structure can be explained by proposing that Ded1 promotes PIC attachment and (especially) subsequent scanning by resolving RNA structures that impede the threading of mRNA in single-stranded conformation through the mRNA binding cleft of the 40S subunit. How can we explain the finding that most mRNAs display an equally strong, but much more uniform dependence on eIF4A? One possibility would be that eIF4A stimulates eIF4G binding to mRNA and 43S PIC attachment to eIF4F·mRNPs primarily by resolving the large ensemble of weaker RNA-RNA interactions involving cap-proximal 5′ UTR nucleotides that occur within all mRNAs and impede both processes. The presence of a strong cap-proximal SL would not increase the requirement for eIF4A either because eIF4A is relatively ineffective in unwinding such stable structures compared to Ded1, or because eIF4G might bind to single-stranded nucleotides straddling the SL and thereby "loop-out" the unresolved duplex. Alternately, the ATP-dependent RNA binding and the RNA- and eIF4G-stimulated ATPase activity of eIF4A may provide an essential function in translation initiation not related directly to removing mRNA secondary structure. It will be interesting to compare the relative importance of eIF4A and Ded1 in attachment of eIF4G and 43S PICs to different native mRNAs in vivo.

Methods

Construction of yeast strains and plasmids

Yeast strains and plasmids used in this study are listed in Supplemental Tables S3 and S4, and were generated as described in Supplemental Material.

Yeast biochemical methods

β-galactosidase activities were assayed in WCEs as described previously (Chiu et al. 2010). To assay *LUC* reporters, cells were disrupted with glass beads in 1× PBS containing two Complete EDTA-free Protease Inhibitor Cocktail Tablets (Roche)/50 mL, and firefly luciferase activities were measured using the Dual-Luciferase Reporter Assay System (Promega) according to the supplier's protocol and normalized to the total protein levels in the extracts.

Polysome profiles, polysome gradient fractionation, RNA isolation, and quantitative RT-PCR

For polysome analysis, strains were cultured under the conditions specified in the Results to A_{600} ~0.8, cycloheximide was added to 50 μg/mL for 5 min prior to harvesting, and WCEs were prepared and resolved by sedimentation through sucrose density gradients, as detailed in the Supplemental Material.

Ribosome footprinting and RNA-seq

Ribosome profiling was conducted essentially as described (Ingolia et al. 2009; Ingolia 2010). Statistical analysis of differences in ribosome footprint or RNA-seq read counts, or TE values, between WT and mutant samples was conducted using DESeq (Anders and Huber 2010). Genes with less than 128 total mRNA reads in the four samples combined (replicates of both WT and mutant strains) were excluded from the calculation of TE values.

Data access

Sequencing data from this study have been submitted to the NCBI Gene Expression Omnibus (GEO; http://www.ncbi.nlm.nih.gov/geo/) under accession number GSE66411.

References

Abaeva IS, Marintchev A, Pisareva VP, Hellen CU, Pestova TV. 2011. Bypassing of stems versus linear base-by-base inspection of mammalian mRNAs during ribosomal scanning. *EMBO J* **30:** 115–129.

Anders S, Huber W. 2010. Differential expression analysis for sequence count data. *Genome Biol* **11:** R106.

Beckham C, Hilliker A, Cziko AM, Noueiry A, Ramaswami M, Parker R. 2008. The DEAD-box RNA helicase Ded1p affects and accumulates in *Saccharomyces cerevisiae* P-bodies. *Mol Biol Cell* **19:** 984–993.

Berthelot K, Muldoon M, Rajkowitsch L, Hughes J, McCarthy JE. 2004. Dynamics and processivity of 40S ribosome scanning on mRNA in yeast. *Mol Microbiol* **51:** 987–1001.

Blum S, Schmid SR, Pause A, Buser P, Linder P, Sonenberg N, Trachsel H. 1992. ATP hydrolysis by initiation factor 4A is required for translation initiation in *Saccharomyces cerevisiae*. *Proc Natl Acad Sci* **89:** 7664–7668.

Chiu WL, Wagner S, Herrmannova A, Burela L, Zhang F, Saini AK, Valasek L, Hinnebusch AG. 2010. The C-terminal region of eukaryotic translation initiation factor 3a (eIF3a) promotes mRNA recruitment, scanning, and, together with the eIF3j and the eIF3b RNA recognition motif, selection of AUG start codons. *Mol Cell Biol* **30:** 4415–4434.

Chuang RY, Weaver PL, Liu Z, Chang TH. 1997. Requirement of the DEAD-Box protein ded1p for messenger RNA translation. *Science* **275:** 1468–1471.

de la Cruz J, Iost I, Kressler D, Linder P. 1997. The p20 and Ded1 proteins have antagonistic roles in eIF4E-dependent translation in *Saccharomyces cerevisiae*. *Proc Natl Acad Sci* **94:** 5201–5206.

Geissler R, Golbik RP, Behrens SE. 2012. The DEAD-box helicase DDX3 supports the assembly of functional 80S ribosomes. *Nucleic Acids Res* **40:** 4998–5011.

Hilliker A, Gao Z, Jankowsky E, Parker R. 2011. The DEAD-box protein Ded1 modulates translation by the formation and resolution of an eIF4F-mRNA complex. *Mol Cell* **43:** 962–972.

Hinnebusch AG. 2014. The scanning mechanism of eukaryotic translation initiation. *Annu Rev Biochem* **83:** 779–812.

Ingolia NT. 2010. Genome-wide translational profiling by ribosome footprinting. *Methods Enzymol* **470:** 119–142.

Ingolia NT, Ghaemmaghami S, Newman JR, Weissman JS. 2009. Genome-wide analysis in vivo of translation with nucleotide resolution using ribosome profiling. *Science* **324:** 218–223.

Kertesz M, Wan Y, Mazor E, Rinn JL, Nutter RC, Chang HY, Segal E. 2010. Genome-wide measurement of RNA secondary structure in yeast. *Nature* **467:** 103–107.

Kozak M, Shatkin AJ. 1977. Sequences and properties of two ribosome binding sites from the small size class of reovirus messenger RNA. *J Biol Chem* **252:** 6895–6908.

Lai MC, Lee YH, Tarn WY. 2008. The DEAD-box RNA helicase DDX3 associates with export messenger ribonucleoproteins as well as tip-associated protein and participates in translational control. *Mol Biol Cell* **19:** 3847–3858.

Lawless C, Pearson RD, Selley JN, Smirnova JB, Grant CM, Ashe MP, Pavitt GD, Hubbard SJ. 2009. Upstream sequence elements direct post-transcriptional regulation of gene expression under stress conditions in yeast. *BMC Genomics* **10:** 7–26.

Lazarowitz SG, Robertson HD. 1977. Initiator regions from the small size class of reovirus messenger RNA protected by rabbit reticulocyte ribosomes. *J Biol Chem* **252:** 7842–7849.

Lee CS, Dias AP, Jedrychowski M, Patel AH, Hsu JL, Reed R. 2008. Human DDX3 functions in translation and interacts with the translation initiation factor eIF3. *Nucleic Acids Res* **36:** 4708–4718.

Linder P, Jankowsky E. 2011. From unwinding to clamping—the DEAD box RNA helicase family. *Nat Rev Mol Cell Biol* **12:** 505–516.

Mitchell SF, Walker SE, Algire MA, Park EH, Hinnebusch AG, Lorsch JR. 2010. The 5′-7-methylguanosine cap on eukaryotic mRNAs serves both to stimulate canonical translation initiation and block an alternative pathway. *Mol Cell* **39:** 950–962.

Parsyan A, Shahbazian D, Martineau Y, Petroulakis E, Alain T, Larsson O, Mathonnet G, Tettweiler G, Hellen CU, Pestova TV, et al. 2009. The helicase protein DHX29 promotes translation initiation, cell proliferation, and tumorigenesis. *Proc Natl Acad Sci* **106:** 22217–22222.

Pestova TV, Kolupaeva VG. 2002. The roles of individual eukaryotic translation initiation factors in ribosomal scanning and initiation codon selection. *Genes Dev* **16:** 2906–2922.

Pestova TV, Hellen CUT, Shatsky IV. 1996. Canonical eukaryotic initiation factors determine initiation of translation by internal ribosomal entry. *Mol Cell Biol* **16:** 6859–6869.

Pestova TV, Borukhov SI, Hellen CUT. 1998. Eukaryotic ribosomes require initiation factors 1 and 1A to locate initiation codons. *Nature* **394:** 854–859.

Pisareva VP, Pisarev AV, Komar AA, Hellen CU, Pestova TV. 2008. Translation initiation on mammalian mRNAs with structured 5′UTRs requires DExH-box protein DHX29. *Cell* **135:** 1237–1250.

Ringner M, Krogh M. 2005. Folding free energies of 5′-UTRs impact post-transcriptional regulation on a genomic scale in yeast. *PLoS Comput Biol* **1:** e72.

Rogers GW Jr, Komar AA, Merrick WC. 2002. eIF4A: the godfather of the DEAD box helicases. *Prog Nucleic Acid Res Mol Biol* **72:** 307–331.

Rouskin S, Zubradt M, Washietl S, Kellis M, Weissman JS. 2014. Genome-wide probing of RNA structure reveals active unfolding of mRNA structures *in vivo*. *Nature* **505:** 701–705.

Schutz P, Bumann M, Oberholzer AE, Bieniossek C, Trachsel H, Altmann M, Baumann U. 2008. Crystal structure of the yeast eIF4A-eIF4G complex: an RNA-helicase controlled by protein–protein interactions. *Proc Natl Acad Sci* **105:** 9564–9569.

Shih JW, Tsai TY, Chao CH, Wu Lee YH. 2008. Candidate tumor suppressor DDX3 RNA helicase specifically represses cap-dependent translation by acting as an eIF4E inhibitory protein. *Oncogene* **27:** 700–714.

Soto-Rifo R, Rubilar PS, Limousin T, de Breyne S, Decimo D, Ohlmann T. 2012. DEAD-box protein DDX3 associates with eIF4F to promote translation of selected mRNAs. *EMBO J* **31:** 3745–3756.

Svitkin Y, Pause A, Haghighat A, Pyronnet S, Witherell GW, Belsham G, Sonenberg N. 2001. The requirement for eukaryotic initiation factor 4A (eIF4A) in translation is in direct proportion to the degree of mRNA 5′ secondary structure. *RNA* **7:** 382–394.

Wan Y, Qu K, Ouyang Z, Kertesz M, Li J, Tibshirani R, Makino DL, Nutter RC, Segal E, Chang HY. 2012. Genome-wide measurement of RNA folding energies. *Mol Cell* **48:** 169–181.